ELSEVIER

Ceramics International 33 (2007) 595–600

CERAMICS INTERNATIONAL

www.elsevier.com/locate/ceramint

Micro-Raman spectroscopic investigation of rare earth-modified lead zirconate titanate ceramics

S.R. Shannigrahi *, S. Tripathy

Institute of Materials Research and Engineering, 3 Research Link, 117602 Singapore, Singapore

Received 1 August 2005; received in revised form 5 October 2005; accepted 21 November 2005
Available online 17 February 2006

Abstract

Rare earth-modified lead zirconate titanate (PRZT) ceramics [R/Zr/Ti = 8/60/40; R = La and Pr] are prepared by a sol–gel technique. Substantial changes in the dielectric, ferroelectric and piezoelectric properties are observed between La- and Pr-modified PZT ceramics. To correlate the observed differences in the electrical properties with structural modifications, temperature-dependent Raman scattering measurements have been carried out. Significant asymmetric phonon line broadening with a noticeable downward shift has been observed for peaks associated with E and A_1 symmetry, particularly in Pr-modified PZT when the sample temperature increases. In addition, low-temperature Raman spectra of Pr-modified PZT show splitting of the A_1(1TO) mode and appearance of the sub-peak structures. Such sub-peak structures arising around A_1(1TO) mode could be due to the presence of thermodynamically stable defect-impurity complexes.

Keywords: Raman spectroscopy; Lead zirconate titanate (PZT); La- and Pr-doped PZT

1. Introduction

Lead zirconate titanate [$Pb(Zr,Ti)O_3$; PZT] ceramics is one of the major materials of interest for several device applications as well as for academic research [1–3]. It has been observed that their properties can easily be tailored by substituting ions at the A and/or B sites of the ABO_3 perovskite structure [4–6]. Among these research activities, lanthanum (La) doping (at A-sites) has proven it to be the most successful one for several applications [7,8]. However, depending on the applications, other rare earth dopants are equally important. In this regard, praseodymium (Pr) can also be selected as a probable modifier/dopant to tune the electrical properties of the modified ceramics. In literature, studies on Pr-doped PZT are rather limited [9]. To correlate structure–property relationship in rare earth-doped $Pb(Zr,Ti)O_3$ (PRZT) based ferroelectric materials, micro-Raman scattering technique has been used to probe the soft lattice modes and phase transitions. It has been well established that the soft mode spectroscopy has allowed researchers to investigate the phase transition phenomena (e.g. transition from ferroelectric to paraelectric) in bulk ceramics and thin films prepared by various techniques [10–15]. The Raman peaks can be well correlated with the dielectric properties using the well-known Cochran's soft mode formalism [16].

Raman technique can also address the anharmonic effects in materials, and in some cases, it is a valuable tool to characterize the presence of impurity and lattice disorder through observation of local vibrational modes and disorder-activated Raman peaks. Presence of high defect density and impurity can lead to a relaxation of the phonon wave vector selection rule ($q = 0$) and appearance of Raman peaks and silent modes from different symmetry points of Brillouin zone. In this context, we have explored the structure–property relationship in rare earth-doped PZT ceramics using temperature-dependent Raman scattering. Substantial changes in the electrical properties have been observed between La-modified PZT (PLZT) and Pr-modified PZT (PPZT) ceramics. Micro-Raman probing in Pr-doped ceramics shows the appearance of sub-peak structures around A_1(1TO) phonon mode, which can be associated with thermodynamically stable defect-impurity complexes.

2. Experimental

Ceramic specimens of $Pb(Zr_{0.60}Ti_{0.40})O_3$ (PZT), $Pb_{0.92}La_{0.08}(Zr_{0.60}Ti_{0.40})_{0.98}O_3$ (PLZT), and $Pb_{0.92}Pr_{0.08}(Zr_{0.60}Ti_{0.40})_{0.98}O_3$ (PPZT) were prepared using a sol–gel technique. The precursors

* Corresponding author. Fax: +65 68720785.
E-mail address: santi-s@imre.a-star.edu.sg (S.R. Shannigrahi).

0272-8842/$32.00
doi:10.1016/j.ceramint.2005.11.015

used were lead acetate trihydrate, lanthanum acetate hexahydrate, praseodymium acetate hexahydrate, zirconium propoxide, and titanium isopropoxide. For the individual PZT, PLZT, and PPZT sol preparations, first of all, stoichiometric amount of corresponding (i) lead acetate, (ii) lead acetate and lanthanum acetate hexahydrate, and (iii) lead acetate and praseodymium acetate hexahydrate were dissolved separately in acetic acid in the ratio of 2 g of salt in 1 ml acid and were heated at 110 °C for half an hour to remove the water content, and cooled down to 80 °C. Then stoichiometric amount of zirconium propoxide followed by titanium isopropoxide were added to the solutions in stirring conditions. A small amount of distilled water was added to get the final sol. The sol was kept at 60 °C for 24 h to get the clear transparent gel. The gel was then dried at 100 °C in a controlled oven for 72 h and then a light brown powder was obtained. The oven dried powdered gel was calcined at 550 °C for 15 h. The powder was cold pressed into disks (pellets) using a uniaxial hydraulic press. The pellets were then sintered for 6 h at 1150 °C. In order to prevent PbO loss or vaporization during sintering, an equilibrium PbO vapor pressure was established with $PbZrO_3$ as setter and placing everything inside a covered platinum crucible to maintain the stoichiometry of the compounds.

Crystalline quality of the ceramic specimens was studied by X-ray diffraction (XRD). Microstructures of the samples were analysed by field emission scanning electron microscopy (FE-SEM). Dielectric constant (ε) and dielectric loss ($\tan\delta$) of the samples as a function of temperature (300–650 K) at frequency 10^4 Hz, were obtained using a GR 1620 AP capacitance measuring assembly. Polarisation-electric field (P-E) loops of the samples were recorded using a dual trace oscilloscope attached to the modified Sawyer and Tower circuit. Micro-Raman measurements were carried out using the 514.5 nm line of an argon ion laser as an excitation source. The scattered light was dispersed through a JY-T64000 triple monochromator system attached to a liquid nitrogen cooled charge coupled device (CCD). The entrance slit width in the Raman set up was kept at 50 μm and the use of 2400 gr/mm gratings gives an spectral resolution of 0.2 cm^{-1} with a spatial resolution of about 1.0 μm. For low-temperature measurements, the samples were kept in a liquid nitrogen microscope cryostat (OXFORD Microstat^N), which is placed under the microscope of the Raman system. The temperature was measured with accuracy better than ±0.1 K. In order to obtain the true intrinsic line width of the phonon modes, the instrumental line width was deconvoluted from the experimentally obtained values. The errors in the Raman peak frequency and linewidth were ≤0.2 cm^{-1}.

3. Results and discussion

To probe the structural and crystalline quality of these ceramics, room temperature XRD measurements were carried out on sintered specimens. XRD spectra of PZT, PLZT, and PPZT samples in Fig. 1(a) show the formation of single-phase compounds. All the reflection peaks were indexed and lattice parameters were determined and refined using a least square regression method in PowdMult. According to the room

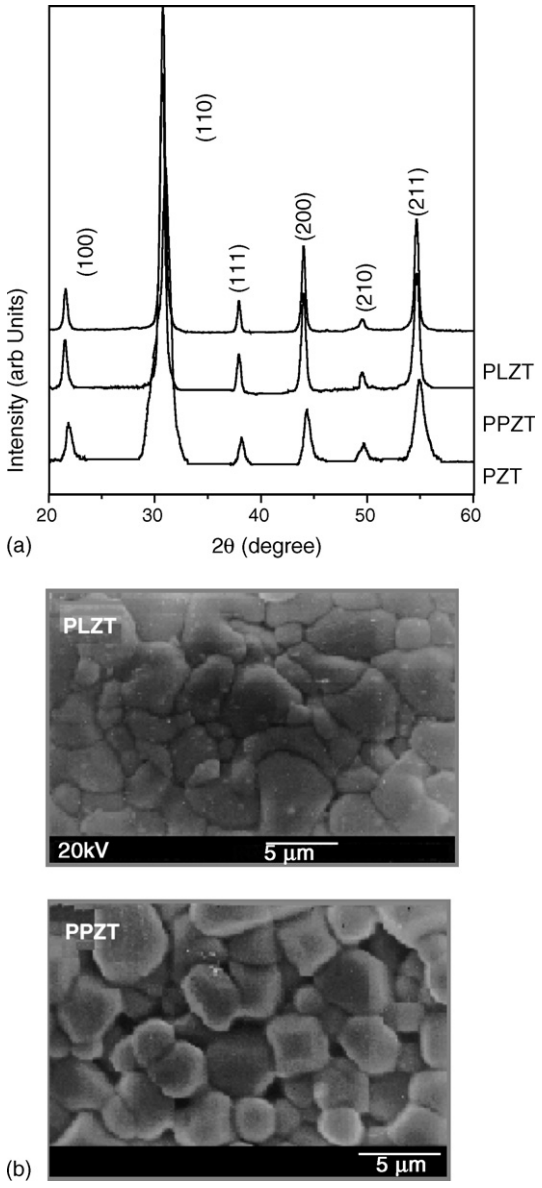

Fig. 1. (a) XRD spectra of PZT, PLZT, and PPZT ceramics and (b) SEM micrographs of these samples.

temperature phase diagram of PZT ceramics for our studied composition, a rhombohedral phase is expected [1]. Compared to pure PZT, a small amount of shift is observed in the peak positions indicating a small change in the lattice parameters in PLZT and PPZT. The lattice parameters estimated for these compounds are shown in Table 1. From the XRD analyses, we conclude that the PLZT and PPZT compounds belong to the tetragonal phase at room temperature, which also supports the existing phase diagram for this particular PLZT and PPZT compositions. SEM micrographs of the PLZT and PPZT samples are shown in Fig. 1b. It can be seen that the grain distribution is almost uniform at the surface of both the samples and we did not observe any significant changes in the microstructural behaviour with doping. The average grain size estimated from SEM is also given in Table 1.

We have also investigated the temperature variation of dielectric constant (ε) at 10^4 Hz for all these samples. The

Table 1
Lattice parameters, dielectric, and ferroelectric parameters of the PZT, PPZT, and PLZT ceramics.

Sample	C.S.	Cell parameters			ε_{max} (10 kHz)	tan δ (10 kHz)	T_c (K)	P_r (μC/cm^2)
		a (Å)	c (Å)	α (°)				
PLZT	T	4.005	4.010	–	18924	0.016	430	17.90
PPZT	T	4.064	4.095	–	2367	0.086	330	4.0
PZT	R	4.133	–	89.75	27607	0.049	636	10.16

C.S.: crystal structure; T: tetragonal; R: rhombohedral.

remnant polarisation (P_r) and coercive field (E_c) were determined from the hysteresis loop. It is observed that the hysteresis loop at 300 K is a memory type in all the samples. From the temperature dependence of E_c and P_r, we have observed that the coercive field shows a linear function with temperature at the Curie point, whereas polarisation appears to be quadratic; both relations indicate a second-order phase transition at T_c. This is also supported by our observations of the temperature gradient of the reciprocal dielectric constant, where at low and high temperature, the gradient is about 2:1 for this composition [17]. All these results suggest that the phase transition is of second order for this composition of PLZT [18,19]. The values of E_c and P_r at 300 K are shown in Table 1. From these observations, it is clear that PLZT shows a much higher dielectric constant ($\sim 1.89 \times 10^4$) and T_c (430 K), compared to the dielectric constant (2.3×10^3) and T_c (330 K) of PPZT.

Fig. 2 shows the room temperature Raman spectra of the PZT, PLZT, and PPZT ceramics. The spectrum recorded from a PZT sample is also shown for a comparison. According to the phase diagram, the PZT sample corresponds to the rhombohedral phase. The Raman spectral features in PLZT and PPZT ceramics correspond to the tetragonal phase following the 4 mm (C_{4v}^1) point group symmetry, where the transverse modes of the T_{1u} transformation, i.e. A_1(1TO) + E(1TO), corresponds to soft modes. The lowest wave-number E(1TO) and A_1(1TO) phonons in the spectra originate from Pb ions vibrating against Zr/TiO_6 octahedra. In addition to these peaks, E(1LO) and higher order modes along with some combinational modes are also observed in the spectra (Fig. 2) recorded from PLZT samples.

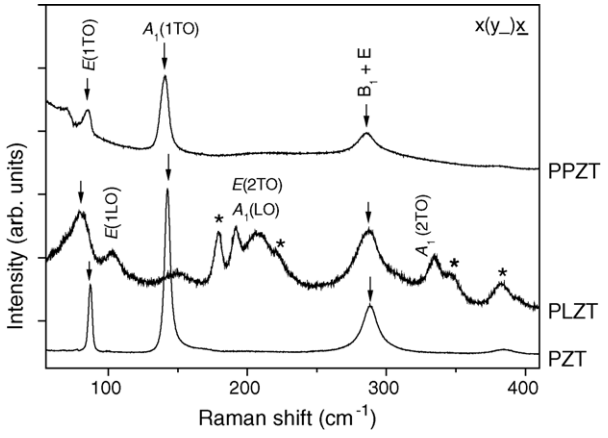

Fig. 2. Room temperature Raman spectra of the PZT, PLZT, and PPZT ceramics. The asterisks marked in the spectrum recorded from PLZT represent combination or coupling of TO modes with Raman active acoustic/optic or local modes.

In the case of such polycrystalline ceramics, the directions of the phonon wave vectors ($\boldsymbol{q}$) are randomly distributed with respect to the crystallographic axes. However, existence of long-range ferroelectric ordering in these materials can follow selection rules in different polarization geometries. Because of the polarization mixing and random distributions of the $\boldsymbol{q}$ directions, Raman line broadening can occur in the tetragonal phase. However, Raman spectral characteristics show that the samples are somewhat preferentially oriented and resemble spectra of single crystalline material. In our case, Raman spectra are recorded with a high numerical aperture objective lens (100×, NA: 1.25) with a spot size of about 1.0 μm, hence, Raman lineshape appears from the surface and cross section of individual grains. As a result, Raman linewidth from these studied samples is much narrower when compared to spectra reported in Ref. [20] due to improved lateral resolution and orientation effects. Observation of these peaks clearly demonstrates the Raman selection rules of zone center optical phonons for PZT based materials.

When compared to spectra recorded from PZT, the soft E(1TO) mode recorded from PLZT ceramics show an asymmetric line broadening and a noticeable downward shift. The observed line broadening can be attributed to the doping induced disorder and compositional fluctuation arising from a random distribution of Ti and Zr cations over the B-site sublattices. Upon doping by La or Pr, these ionic species compete for a given site in PZT and destroy the translational invariance. Since the Raman mode frequency is related to the force constant and the reduced mass, the observed downward shift of the mode frequencies in the PRZT samples reflects either a decrease or an increase of partial replacement of more ionic species. These effects could lead to corresponding changes in the Raman spectrum, such as appearance of phonons from other points of Brillouin zone and splitting of the degenerate $B_1 + E$ silent modes. Higher-order phonon scattering involving such process also leads to appearance of higher-order combinational modes. The asterisks marked in the spectrum recorded from PLZT sample represents coupling of the A_1 and E phonon mode with other zone-boundary optic, acoustic or local phonon modes. However, in PPZT sample, the A_1(1TO) mode is much stronger compared to other symmetric modes and we could only detect A_1(1TO), E(1TO), and silent $B_1 + E$ mode.

To further explore the nature of the scattering processes and anharmonic effects, we have carried out temperature-dependent

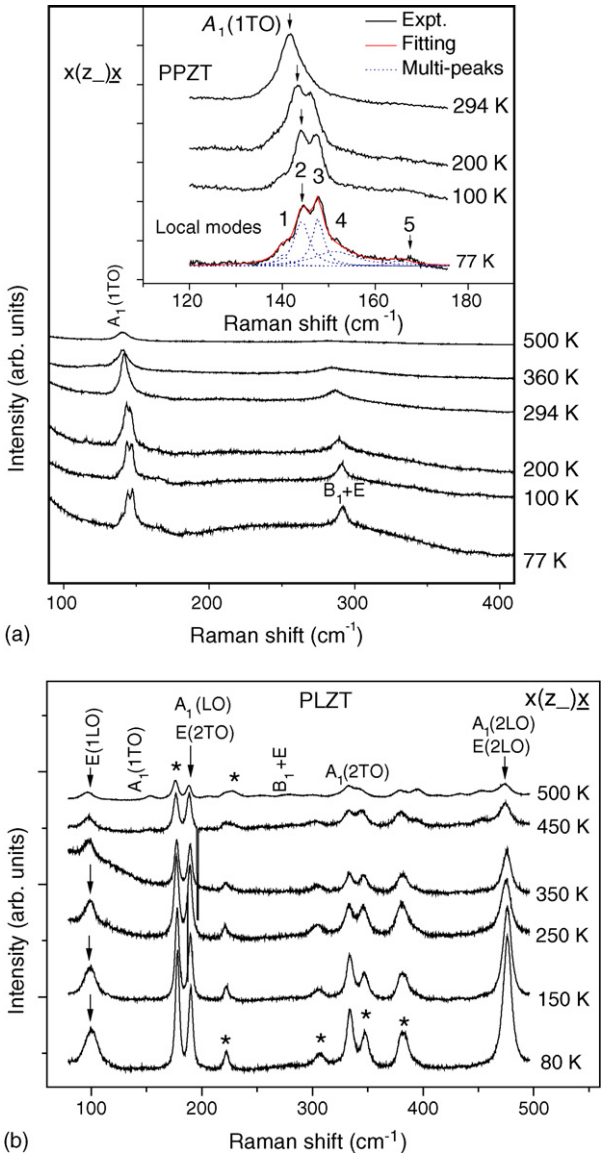

Fig. 3. Temperature-dependent Raman spectra of the (a) PPZT and (b) PLZT ceramics. Inset in (a) shows the multiple peaks observed around A_1(1TO) phonon peak in Pr-doped PZT. The spectrum obtained at 77 K is fitted by multiple Lorenztian functions.

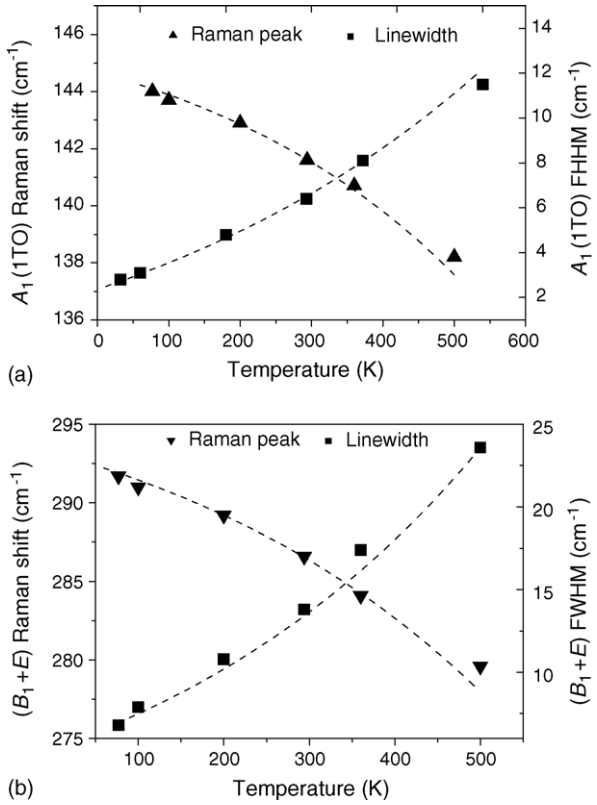

Fig. 4. Raman peak shift and linewidth (FWHM) as a function of temperature in PPZT sample. (a) Temperature variation of A_1(1TO) mode and (b) temperature variation of $B_1 + E$ mode. The fitting of the spectral peak and linewidth are shown as dashed lines.

Raman scattering measurements in PLZT and PPZT samples in the temperature range 77–500 K and the spectra recorded under a specific scattering geometry are shown in Fig. 3. The Raman peak position and FWHM of the peaks were obtained by Lorentzian fitting of the line shape. The contribution of the slit broadening was also taken into account and the true line width of the Raman lines were extracted from the extrapolation to zero-slit width. In PLZT specimen, due to anharmonic effects, the mode peak frequency shows softening as well as substantial broadening with an increase in the sample temperature. As temperature increases toward the transition temperature, all the modes show a substantial decrease in peak intensity. The observed downward shift and broadening of the mode frequency with an increase in temperature can support the phase transition processes [5,21].

The deviation of phase transition temperature as evidenced by dielectric studies can be due to a relaxor-type behavior in this system, where short-range structural ordering due to formation of vacancy-impurity complexes could influence the Raman mode intensity. At higher temperature, we have observed a significant downward shift and broadening for the A_1(LO)/E(2TO) modes from PLZT. The combinational modes or the local modes, associated with defects or impurities (marked as asterisks in Fig. 3b), show appearance of broad shoulders and tail above the macroscopic tetragonal-cubic transition temperature. This indicates that short-ranged clusters with tetragonal 4 mm symmetry are still distributed over the globally cubic matrix at a temperature substantially higher than the macroscopic transition temperature. As expected, above 500 K, these clusters may also undergo phase transitions leading to a complete break up of tetragonal symmetry.

Since Pr-doping in PZT shows a substantial decrease of the values of dielectric properties, we have tried to correlate this observation through temperature-dependent Raman study. In Fig. 4, we have also shown the variation of the Raman peak and FWHM as a function of temperature for major intense Raman peaks observed from PPZT sample. At higher temperature, the A_1(1TO) phonon lineshape in PPZT is found to be more asymmetric in nature compared to the case of PZT. Such lineshape in $PbTiO_3$ crystals is generally attributed to the anharmonic nature of the effective interatomic potential or due

to presence of thermodynamically stable defect complexes [22–24]. The most significant result is obtained from 77 K A_1(1TO) Raman peak of PPZT near 144 cm^{-1}. The peak shows splitting of the mode into sub-peak structures. In addition, some other broad peaks appear around A_1(1TO) phonon peaks.

According to the anharmonicity model proposed by Foster et al. [25], the A_1(1TO) mode consists of four distinct sub-peaks in $PbTiO_3$ crystals, where each subpeak corresponds to the vibrational transition from one quantum state to its neighboring quantum states. We have carried out a multi-Lorenztain fitting of these modes observed from PPZT specimens at low temperature. Each sub-peak is labeled and the fitting is shown in the inset of Fig. 3a. The splitting of the peak is clearer at 77 K, since much narrower Raman linewidth is expected. If we consider the anharmonic model, the major sub-peak of the A_1(1TO) observed at 77 K should be the first sub-peak, and with an increase in quantum number, the other peaks should show broadening due to shorter phonon lifetimes.

From temperature-dependent measurements, we found the softening behavior of all the modes as a function of temperature. The peak frequency and FWHM of the major sub-peak as a function of the temperature is illustrated in Fig. 4a. As the sample temperature approached the phase-transition point, there is a substantial decrease in the peak frequency with broadening. Also the spacing between the peak structures is not regular at 77 K. It is found that the spacing between the peaks decreases with increase in the sample temperature. If we consider that only the anharmonic model, then spacing between adjacent subpeaks will increase as temperature rises. Moreover, there is a relative intensity change observed for the two major peaks at 143 and 147 cm^{-1}. Lower the temperature, stronger is the mode near 143 cm^{-1}. But at 77 K, the mode at 147 cm^{-1} shows higher intensity. The mode observed at the higher energy side of the major sub-peak also shows a substantial decrease in the spacing with temperature. Therefore, we believe that some other mechanism is involved that has led to the splitting of the A_1(1TO) peak or appearance of additional modes due to Pr-doping in PZT. Another possible effect may arise from strain fields due to change in local crystal symmetry with Pr-doping. Similar observation were reported for the case of $BaTiO_3$ where splitting of the A_1(2TO) occurs due to strain fields [26]. Such effects can be ignored in our samples, since these materials are polycrystalline in nature and existence of strain field can dominate only in the single crystalline films.

We have also carried out temperature dependent Raman measurements on the PZT specimens. No peak splitting of the A_1(1TO) or E(TO) mode occurred at 77 K. Compared to the observed changes of Raman peaks in PPZT with respect to PZT ceramics, the following mechanisms can lead to appearance of these sub-peaks in the Raman spectrum at lower temperature: change in phonon dispersion at the zone center due to existence of Pr in PZT, coupling of zone center A_1(1TO) mode with a low energy phonons or observation of local modes related to Pr-impurity. Taking into account of the temperature dependent Raman intensity profiles, we conclude that there is no multiple phonon scattering phenomena that can give rise additional peaks near A_1(1TO) phonon. Moreover, considering phonon dispersion curves, we can rule out the possibility of a coupling of this soft mode with an impurity peak or acoustic phonons. The last possible reason could be the observation of local vibrational modes related to Pr-dopant or stable defect-impurity complexes. These localized modes can be viewed as modified A_1(1TO) modes due to Pr-doping in PZT. We believe that the presence of Zr/Ti and Pr at sub-lattice sites could give rise to multiple sub-peaks around A_1(1TO) mode due to presence of thermodynamically stable defect-impurity complexes. Since these modes are showing A_1-like characteristics, it can be concluded that at low temperature, the local frozen fluctuations caused by these stable defect-impurity complexes are confined to a very small region around the Pr-impurity center. With an increase in temperature, the correlation between local polarizations increases sharply and external perturbations gives rise to line broadening. Such effects were also observed for the sub-peak structures of Ba-doped $PbTiO_3$ single crystals as reported by Jang and co-workers [24,27]. Observation of such local modes clearly suggest that the local Curie point of the defective region would be significantly lower than that of the intrinsic PZT regions, which are free from lattice defects or impurities. The polarization correlation will be initiated at the defect-impurity sites. This would further lead to an increase in the correlation length and under influence of this long-range polarization correlation, the phase transition temperature will be much lower when compared to pure PZT ceramics.

From XRD observations, we have found that the tetragonality (c/a) increases in PPZT compared to PLZT. In Pr-doped PZT, the longer distance between the center ion and its nearest neighbors softens the vibration amplitude of center ion in a different way when compared to PLZT, and such effect decreases the contribution from anharmonic effects. Consequently, the dielectric constant would show substantial change due to presence of defect-impurity complexes in PPZT. This means that the amount of remnant polarization is decreased with the incorporation of Pr, resulting in the significant reduction of dielectric constant. Such effects could be due to a lowering of c-axis crystal symmetry in PPZT ceramic grains. All these observations can be correlated with the Raman data, where presence of thermodynamically stable defects in PPZT could lead to observation of sub-peak structures and anomalous A_1(1TO) line shape.

4. Conclusions

We have investigated both room temperature and temperature dependent vibrational properties of rare earth-doped PZT ceramics using micro-Raman scattering and tried to correlate the structural properties with the observed changes in the dielectric and ferroelectric properties. Raman spectra recorded from PPZT sample shows substantial line broadening and phonon softening with the increase of sample temperature. Furthermore, observation of sub-peak structures around A_1(1TO) phonon in PPZT shows the presence of stable defect-impurity complexes. These complexes can be formed

due to Pr-doping and give rise to local vibrational modes around A_1(1TO) phonon peak, and as a result the A_1(1TO) soft phonon mode shows anomalous lineshape.

References

[1] M.E. Lines, A.M. Glass, Principles and Applications of Ferroelectrics and Related Materials, Oxford University Press, 1977.
[2] A.D.E. Lakeman, D.A. Payne, J. Am. Ceram. Soc. 75 (1992) 3091.
[3] H.J. Kim, S.H. Oh, H.M. Jang, Appl. Phys. Lett. 75 (1999) 3195.
[4] J.D. Freire, R.S. Katiyar, Phys. Rev. B 37 (1988) 2074.
[5] Z. Ujma, J. Handerek, H. Hassan, G.E. Kungel, M.J. Pawelczyk, J. Phys. Condens. Matter 7 (1995) 895.
[6] M.E. Marssi, R. Farhi, D. Viehland, J. Appl. Phys. 81 (1997) 355.
[7] (a) G.H. Haertling, C.E. Land, J. Am. Ceram. Soc. 54 (1971) 1; (b) G.H. Haertling, J. Am. Ceram. Soc. 54 (1971) 303.
[8] E.T. Keve, K.L. Bye, J. Appl. Phys. 46 (1975) 810.
[9] S.R. Shannigrahi, R.N.P. Choudhary, H.N. Acharya, J. Mater. Sci. Lett. 18 (1999) 345.
[10] J.F. Scott, Rev. Mod. Phys. 46 (1974) 83.
[11] G. Burns, B.A. Scott, Phys. Rev. B 7 (1973) 3088.
[12] P.S. Dobal, R.S. Katiyar, J. Raman Spectrosc. 33 (2002) 405.
[13] A.G. Souza Filho, K.C.V. Lima, A.P. Ayala, I. Guedes, P.T.C. Freire, F.E.A. Melo, J. Mendes Filho, E.B. Araujo, J.A. Eiras, Phys. Rev. B. 66 (2002) 132107.
[14] E.B. Araujo, K. Yukimitu, J.C.S. Moraes, L.H.Z. Pelaio, J.A. Eiras, J. Phys. Condens. Matter 15 (2003) 4851.
[15] A.G. Souza Filho, K.C.V. Lima, A.P. Ayala, I. Guedes, P.T.C. Freire, J. Mendes Filho, E.B. Araujo, J.A. Eiras, Phys. Rev. B. 61 (2000) 14283.
[16] W. Cochran, Adv. Phys. 9 (1960) 387.
[17] S.R. Shannigrahi, R.N.P. Choudhury, H.N. Acharya, Mater. Chem. Phys. 58 (1999) 204.
[18] W. Eysel, R.W. Wolfe, R.E. Newnham, J. Am. Ceram. Soc. 56 (1972) 185.
[19] S.M. Pilgrim, A.E. Sutherland, S.R. Winzer, J. Am. Ceram. Soc. 73 (1990) 3122.
[20] K.C.V. Lima, A.G. Souza Filho, A.P. Ayala, J. Mendes Filho, P.T. Freire, F.E.A. Melo, E.B. Araujo, J.A. Eiras, Phys. Rev. B 63 (2001) 184105.
[21] M.E. Marssi, R. Farhi, X. Dai, A. Morell, D. Viehland, J. Appl. Phys. 80 (1996) 1079.
[22] D. Fontana, H. Idrissi, G.E. Kungel, K. Wojcik, J. Phys. Condens. Matter 3 (1991) 8695.
[23] C.M. Foster, Z. Li, M. Grimsditch, S.K. Chan, D.J. Lam, Phys. Rev. B 48 (1993) 10160.
[24] S.M. Cho, H.M. Jang, T.Y. Kim, Phys. Rev. B 64 (2001) 014103.
[25] C.M. Foster, M. Grimsditch, Z. Li, V.G. Karpov, Phys. Rev. Lett. 71 (1993) 1258.
[26] M. Osada, M. Kakihana, S. Wada, T. Noma, W.S. Cho, Appl. Phys. Lett. 75 (1999) 3393.
[27] S.M. Cho, J.H. Park, H.M. Jang, J. Appl. Phys. 94 (2003) 1948.